

# An Evaluation of Suspended Sediment Concentration on Von Karman's Constant

Michael L. Hackett

Department of Mathematics, Physics and Statistics,  
University of Guyana, Tain Campus, Guyana

**Abstract:-** This paper investigates the relationship between flow velocity, flow height, and von Karman's constant,  $\kappa$ , in a marine environment. It is based on empirical measurements obtained in Western Solent, Southampton, UK. The velocity gradient is explored to understand its relation to bed shear stress and the formation of the benthic boundary in the water column.

The paper explores von Karman's constant as a parameter that characterises the rough-turbulent regime, where shear stress is proportional to the square of the flow velocity. It evaluates  $\kappa$  for the study area and explores whether  $\kappa$  remains constant or varies with suspended sediment concentration.

Results show that the calculated friction velocity and  $\kappa$  are within the expected range, supporting the validity of the Reynolds stress method. The average value of  $\kappa$  obtained is 0.442, slightly higher than the generally accepted value. However, the correlation between  $\kappa$  and suspended sediment concentration is inconclusive, indicating the need for further research.

This paper provides some insights into the dynamics of turbulent flow in a marine environment and sheds some light on the nature of von Karman's constant, emphasising the importance of suspended sediment concentration in understanding flow behaviour near the bed.

**Keywords:-** Acoustic Doppler Current Profiler (ACDP), Autonomous Benthic Recorder (ABR), bed shear stress, benthic boundary, Electromagnet Current Meter (EMCM), friction velocity, Optical Backscatter Sensor (OBS), suspended sediment concentration (SSC), turbidity, Valeport.

## I. INTRODUCTION

It is an empirical fact that when water flows over a stream bed, the horizontal flow velocity is greater when it is further away from the bed and smaller when closer to the bed, becoming zero close to, or in contact with, the bed. This behaviour can be conceptualised as a velocity gradient, that is, a variation of velocity,  $u$ , over a variation of flow height,  $z$ , such that the velocity gradient is related inversely to height and proportionally to flow velocity (Dyer, 1986). It is expressed in calculus notation as:

$$\frac{du}{dz} \propto \frac{u}{z} \quad (1)$$

The existence of the velocity gradient is a direct result of friction between the moving water and the stationary bed. Due to this resistance, when the lowest layer of water moves over the bed, momentum is removed from it and is transferred to the bed, producing a horizontal bed shear stress,  $\tau_0$ , between that layer of water and the bed. By virtue of the molecular viscosity,  $m$ , of water, this shear stress is transmitted from lower layers to upper layers of water, with the flow velocity increasing with flow height and the shear stress decreasing with height.

The velocity gradient is more significant closer to the bed and smaller further away from the bed, and it appears as a manifestation of the bed shear stress, which in turn is caused by the momentum flux from the flow to the bed. The momentum transferred to the bed is then dissipated as energy in the form of eddies, heat, and motion of any movable sediment that may lie on the bed.

The velocity gradient is, therefore, some function of flow velocity, flow height, and bed shear stress. With empirical measurements of  $u$  and  $z$ , a precise knowledge of the nature of this relation will enable predictions to be made for bed shear stress, the height at which the velocity goes to zero, and the nature of the bed and any movable sediment that comprises it (Bagnold, 1973).

## II. SURVEY AREA DESCRIPTION

The survey for this report was done on March 6, 2009, on the coastal vessel R.V. Bill Conway. The survey area was off the mouth of the Beaulieu River in the Western Solent, Southampton – Latitude 50° 46.399 N, Longitude 001° 22.277 W. The time for data and sample collection lasted from 10:13 hours to 14:57 hours, a total time of four hours and forty-four minutes. The depth of water was approximately 5.0 m. Tides predictions for the day were 05:39 hours high, 11:56 hours low, and 18:35 hours high.

## III. RELATION BETWEEN FLOW VELOCITY AND FLOW HEIGHT IN ROUGH TURBULENCE - VON KARMAN'S CONSTANT

Since Equation (1) contains three variables, it cannot be integrated to give a useful relation for marine and estuarine environments where turbulent flows are the norm unless one of the variables is parameterised as a constant. This can be done using experimental observations, which show that when the flow is in the rough-turbulent regime, the shear stress  $\tau$  is proportional to the square of the velocity  $u$ :

$$\tau \propto u^2 \quad (2)$$

(Dyer, 1986)

Also, in rough turbulence, the viscous sub-layer that is present in nearly laminar flow, where Newton's Law of Viscosity ( $\tau = \mu du/dz$ ) holds, becomes negligible; therefore, this Law no longer holds, instead Equation (2) becomes applicable in the near-bed zone. Here, the shear stress is constant and is equal to the bed shear stress,  $\tau_0$ . Dimensionally,  $\tau_0/\rho =$  units of velocity squared, where  $\rho =$  density of water. This quantity is the square of the friction velocity,  $(u^*)^2$ , therefore:

$$\tau_0 = \rho u_*^2 \Rightarrow u_* = \sqrt{\frac{\tau_0}{\rho}} \tag{3}$$

(Bagnold, 1973)

Although  $u_*$  is merely a mathematical symbol for  $\sqrt{(\tau_0/\rho)}$ , it is dimensionally equivalent to the empirical Equation (2). This allows Equation (1) to be expressed for rough-turbulent flow by replacing  $u$  with  $u_*$ , thus:

$$\frac{du}{dz} \propto \frac{u_*}{z} \Rightarrow \frac{du}{dz} \propto \frac{1}{z} \sqrt{\frac{\tau_0}{\rho}} \tag{4}$$

The proportionality is converted to an equation by introducing a constant,  $\kappa$ , in the denominator giving:

$$\frac{du}{dz} = \frac{1}{\kappa z} \sqrt{\frac{\tau_0}{\rho}} \Rightarrow \frac{du}{dz} = \frac{u_*}{\kappa z} \tag{5}$$

where  $\kappa =$  von Karman's constant (Dyer, 1986).

Since the velocity gradient results from the flow to the bed, von Karman's constant expresses the relation between momentum flux to the velocity gradient and the formation of the benthic boundary in the water column. From Equation (5),  $\kappa$  is seen to be a dimensionless number, and it is assumed to

be a constant.

#### IV. DERIVING THE VON KARMAN-PRANDTL EQUATION (LAW OF THE WALL)

Integrating Equation (5) and defining a height  $z_0$  at which velocity is zero for a rough-turbulent flow ( $u = 0$  when  $z = z_0$ ) gives:

$$\int_0^{u(z)} du = \frac{u_*}{\kappa} \int_{z_0}^z \frac{dz}{z} \Rightarrow u(z) = \frac{u_*}{\kappa} \ln\left(\frac{z}{z_0}\right) \tag{6}$$

In log-linear form:  $\ln z = \frac{\kappa}{u_*} u(z) + \ln z_0$  (7)

where  $z_0 =$  roughness length, and  $\kappa$  and  $u_*$  are constants.

Equation (7) is of the form  $y = mx + c$ , where  $y = \ln z$ ,  $m = \kappa/u_*$ ,  $x = u(z)$  and  $c = \ln z_0$ .

Using measured  $z$  values and time-averaged  $u$  values from velocity profiles obtained via Acoustic Doppler Current Profiler (ADCP) data and processed by the software WinRiverII, graphs of Equations (7) can be plotted. A graph of  $\ln z$  on the  $y$ -axis and  $u(z)$  on the  $x$ -axis will give a straight line from which the gradient,  $m$ , can be readily determined using the trend line function in MS Excel. Hence, the ratio,  $m = \kappa/u_*$  can be known.

In exponential form, Equation (7) is written:

$$z = z_0 e^{\frac{\kappa u}{u_*}} \tag{8}$$

A graph of  $z$  versus  $u$  will yield an exponentially increasing curve, which shows the velocity profile of a unidirectional, non-stratified flow as in Figure 1.

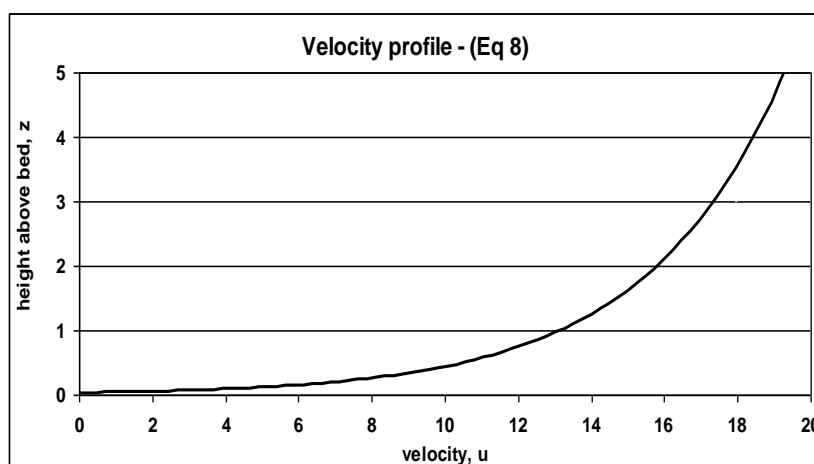


Fig. 1: Graph showing the velocity profile of a unidirectional, non-stratified flow

When this profile is linearised by plotting  $\ln z$  against  $u$ , the linear graph of Equation (7) is obtained as in Figure 2.

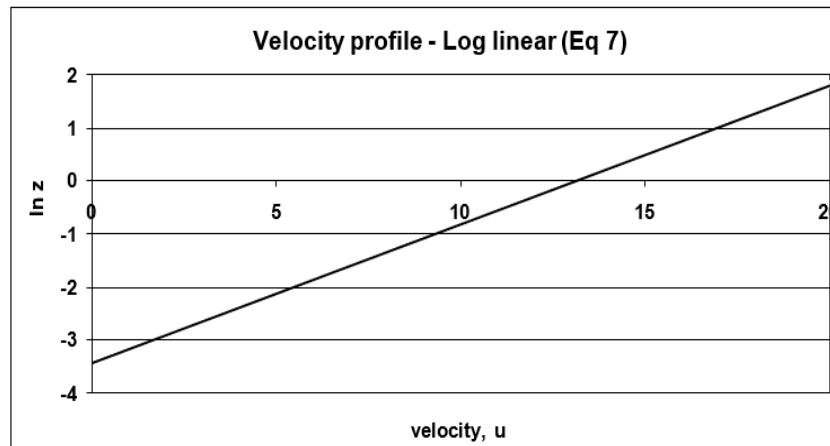


Fig. 2: Graph showing the log linear velocity profile

This graph illustrates the rough turbulence log-linear layer in the near-bed zone (less than 2m above the bed) where the shear stress is constant and is equal to the bed shear stress,  $\tau_0$ .

During a smooth turbulence regime or nearly laminar flow, the viscous sub-layer exists as a thin but significant layer below the log-linear layer. Shear stress is transmitted by molecular viscosity in the viscous sub-layer. However, when rough turbulence predominates, the viscous sub-layer almost disappears, and the log-linear layer extends down to the bed (Leeder, 1982).

In the flow regime of rough turbulence, where inertial forces predominate over viscous forces (implying high Reynolds numbers), von Karman’s constant is made manifest. In this state of turbulence, the transfer of momentum from the flow to the bed and the shear stress exerted by the bed on the flow now happen because of inertial forces of water particles impacting the bed rather than as viscous forces (Bergmann, 1998).

**V. EVALUATION OF  $\kappa$  VALUES**

Once the gradient of the log-linear graph has been evaluated ( $m = k/u^*$ ), the friction velocity  $u^*$  needs to be determined to evaluate  $k$  values. The friction velocity will be found using an adaptation of the Reynolds Stress Method and flow velocity data obtained from the Electromagnet Current Meter (EMCM) on the Valeport, which was deployed at the bed of the survey location.

The EMCM measures  $u$  and  $v$  flow velocities every second in 512-second bursts in the horizontal plane at a measured height of  $z = 0.2$  m above the bed. At this height, it is in the log-linear layer of the benthic boundary where the friction velocity and bed shear stress are constant. The appropriate Reynolds stress is given by:

$$\tau_{xy} = \rho \bar{u}' \bar{v}' \tag{9}$$

where  $u = \bar{u} + u'$  and  $v = \bar{v} + v'$  (Leeder, 1982).

$u, v$ : instantaneous velocities (as measured by the EMCM every second)

$\bar{u}, \bar{v}$ : mean velocities over time

$u', v'$ : instantaneous deviations from the mean

$\bar{u}', \bar{v}'$ : root mean squared deviations.

In the log-linear layer, the Reynolds stress is almost constant and is related to the constant bed shear stress by:

$$\tau_{xy} = \tau_0 \left(1 - \frac{z}{h}\right) \tag{10}$$

where  $h$  = flow depth (Wood, 1981; Cloutier, Amos *et al*, 2006).

The equations for the stresses  $\tau_{xy}$  and  $\tau_0$  are substituted into Equation (10), giving:

$$\rho \bar{u}' \bar{v}' = \rho u_*^2 \left(1 - \frac{z}{h}\right) \Rightarrow u_* \sqrt{\frac{\bar{u}' \bar{v}'}{\left(1 - \frac{z}{h}\right)}} \tag{11}$$

Equation (11) was used in MS Excel to calculate values for  $\bar{u}'$  and  $\bar{v}'$  for every 512-second burst of EMCM data with  $z = 0.2$  m and  $h = \sim 5$  m. From the  $u_*$  value,  $\kappa$  can be calculated using  $\kappa = mu_*$ . The pressure-depth sensor of the Autonomous Benthic Record (ABR) on the Valeport was measured at a height of 0.45 m above the bed, so that will have to be added to the recorded depth to get the true flow depth,  $h$ .

**VI. IS VON KARMAN’S CONSTANT A ROBUST CONSTANT OR A WEAK VARIABLE?**

The generally accepted value of von Karman’s constant for all homogeneous, sediment-free fluids is  $k = 0.4$ . This value can change in a sediment-laden flow (Wood, 1981). Yalin (1972) found that values of  $k$  vary from 0.36 to 0.417 and yet give good agreement with experimental data. If the fluid is non-homogeneous with a high suspended sediment concentration, then the experimental values of von Karman’s “constant” vary.

Bergmann (1998) showed, using pure mathematical methods, that “ $\kappa = \exp(-1) = 0.3678\dots$ ” and that “the result for the value of von Karman constant turns out to be quite a natural constant.”

Dyer (1986) contends that because most studies only measure velocity profiles in the upper part of the flow, they tend to overestimate  $\tau_0$ , resulting in reduced values of  $\kappa$ , some as low as 0.2. He contends this is a “misrepresentation of the physics” since velocity profiles taken closer to the bed yield values of  $\kappa$  not very different from the clear-water value. Soulsby and Dyer (1981) said that the evidence for the reduction of  $\kappa$  in high suspended sediment concentrations is “confused by the separate effect of density stratification caused by the sediment” and that “the reduction of  $\kappa$  may be a misinterpretation.”

There is still some debate over whether  $\kappa$  is a robust constant or a weak variable. If not a ‘true’ constant, then it may vary, however weakly, with the suspended sediment concentration. It is reasonable to assume that the presence of suspended sediments might reduce the coupling of momentum transfer from the flow to the bed during rough turbulence, resulting in a decrease in the value of  $\kappa$ .

**VII. MEASURING SUSPENDED SEDIMENT CONCENTRATION**

The suspended sediment concentration will be determined from analyses of the water and sediment samples taken by the Halley-Smith sand traps and Niskin bottles and turbidity measurements of the Optical Backscatter Sensor (OBS) on the Valeport at the survey location.

Since  $\kappa$  is to be measured for near-bed conditions in the log-linear layer (less than 2 m above the bed), concentrations will be found for the times when the epi-benthic sand traps and near-bed Niskin bottles were deployed. The OBS on the Valeport measured turbidity continuously at the height of 0.4 m above the bed. The corresponding time will be ascertained for velocity profiles from the ADCP, velocity measurements from the EMCM on the Valeport and sediment concentration measurements. This will give a time correspondence between  $\kappa$  values and concentration values.

**VIII. EVALUATING THE RELATION BETWEEN  $\kappa$  AND SUSPENDED SEDIMENT CONCENTRATION**

Measured values of von Karman’s constant against time-corresponding suspended sediment concentrations at similar depths will be plotted on graphs. These will be used to determine the coefficient of determination,  $R^2$ , between  $\kappa$  and suspension concentration. This will indicate the strength of the correlation between  $\kappa$  and suspended sediment concentration to observe the relation between the two quantities.

*A. Tabulated Summary of Results*

Twenty 512-second bursts of data were obtained from the ABR on the Valeport, along with twenty corresponding velocity profiles for the same times extracted from ADCP data. Four data sets were obtained from the epi-benthic sand traps and three sets from the near-bed Niskin bottles. The processed data are summarised in Tables 1 and 2.

Table 1: Tabulated and Processed Results from Valeport – EMCM, OBS, pressure-sensor

| Velocity Profile No. | From  | To    | $\bar{u}'$ (m/s) | $\bar{v}'$ (m/s) | $h$ (m) | $u^*$ (m/s) | $\tau_0$ (N/m <sup>2</sup> ) | Turbidity (V) |
|----------------------|-------|-------|------------------|------------------|---------|-------------|------------------------------|---------------|
| 1                    | 10:38 | 10:46 | 0.005            | 0.009            | 5.44    | 0.007       | 0.049                        | 0.308         |
| 2                    | 10:51 | 10:59 | 0.010            | 0.013            | 5.37    | 0.012       | 0.149                        | 0.302         |
| 3                    | 11:04 | 11:12 | 0.014            | 0.023            | 5.33    | 0.018       | 0.339                        | 0.304         |
| 4                    | 11:17 | 11:25 | 0.017            | 0.025            | 5.29    | 0.021       | 0.459                        | 0.318         |
| 5                    | 11:30 | 11:38 | 0.026            | 0.026            | 5.27    | 0.027       | 0.729                        | 0.307         |
| 6                    | 11:43 | 11:51 | 0.023            | 0.027            | 5.26    | 0.025       | 0.661                        | 0.295         |
| 7                    | 11:56 | 12:04 | 0.032            | 0.039            | 5.28    | 0.036       | 1.340                        | 0.289         |
| 8                    | 12:09 | 12:17 | 0.037            | 0.032            | 5.30    | 0.035       | 1.266                        | 0.402         |
| 9                    | 12:22 | 12:30 | 0.036            | 0.033            | 5.32    | 0.035       | 1.257                        | 0.314         |
| 10                   | 12:35 | 12:43 | 0.031            | 0.035            | 5.33    | 0.034       | 1.182                        | 0.355         |
| 11                   | 12:48 | 12:56 | 0.027            | 0.034            | 5.36    | 0.031       | 0.980                        | 0.324         |
| 12                   | 13:01 | 13:09 | 0.036            | 0.040            | 5.39    | 0.039       | 1.537                        | 0.317         |
| 13                   | 13:14 | 13:22 | 0.043            | 0.047            | 5.42    | 0.045       | 2.114                        | 0.372         |
| 14                   | 13:27 | 13:35 | 0.035            | 0.046            | 5.43    | 0.041       | 1.722                        | 0.436         |
| 15                   | 13:40 | 13:48 | 0.031            | 0.037            | 5.44    | 0.035       | 1.237                        | 0.419         |
| 16                   | 13:53 | 14:01 | 0.037            | 0.036            | 5.46    | 0.037       | 1.394                        | 0.451         |
| 17                   | 14:06 | 14:14 | 0.029            | 0.037            | 5.49    | 0.033       | 1.146                        | 1.212         |
| 18                   | 14:19 | 14:27 | 0.031            | 0.035            | 5.51    | 0.034       | 1.153                        | 2.300         |
| 19                   | 14:32 | 14:40 | 0.026            | 0.024            | 5.52    | 0.025       | 0.647                        | 1.396         |
| 20                   | 14:45 | 14:53 | 0.027            | 0.032            | 5.54    | 0.030       | 0.941                        | 1.646         |

Table 2: Results from Sand Traps & Niskin Bottles and comparing with OBS.

| Epibenthic Sand Trap Sample | OBS File No. | D <sub>50</sub> (mm) | SSC (mg/L)         | OBS Turbidity (V) |
|-----------------------------|--------------|----------------------|--------------------|-------------------|
| E2                          | 4            | 0.283                | 0.0300             | 0.318             |
| E3                          | 10           | 0.245                | 0.0595             | 0.355             |
| E4                          | 14           | 0.085                | 0.0937             | 0.436             |
| E5                          | 18           | n/a                  | 0.1027             | 2.300             |
| Niskin sample               | -            | -                    | Total conc. (mg/L) | -                 |
| NB1                         | 1            | -                    | 9.82               | 0.308             |
| NB2                         | 5            | -                    | 8.20               | 0.307             |
| NB3                         | 10           | -                    | 7.26               | 0.355             |

**B. Non-Calibration of the OBS**

An attempt to calibrate the OBS with suspended sediment concentration (SSC) from the four epi-benthic sand traps

yielded the trend line in Figure 3 below. Since  $R^2 = 0.4396$  is so low for the line, it was not used for further work.

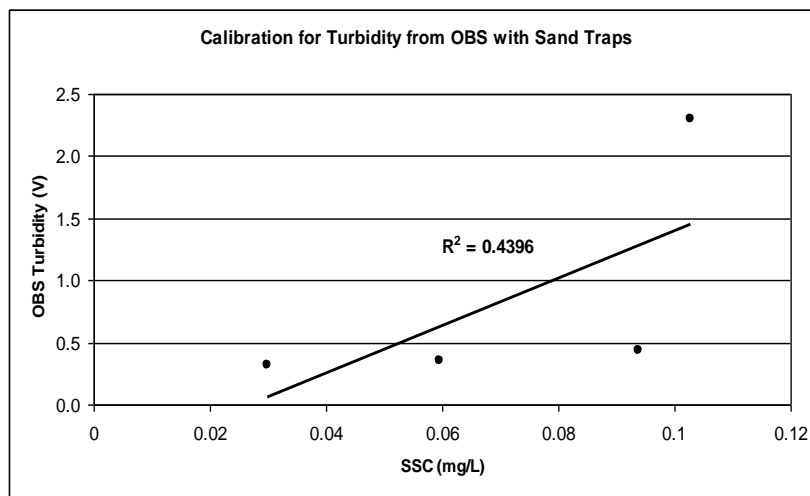


Fig. 3: Graph of OBS Turbidity vs Suspended Sediment Concentration

An attempt to calibrate the OBS using the three near-bed Niskin samples yielded the graph in Figure 4 with a low R<sup>2</sup>. It showed an apparent inverse relation between turbidity and total concentration. This line was also not used for further

work. It was decided to use the OBS voltage values as obtained with the reasonable assumption that there is a linear relation between turbidity measured in volts (V) with suspended sediment concentration measured in mg/L.

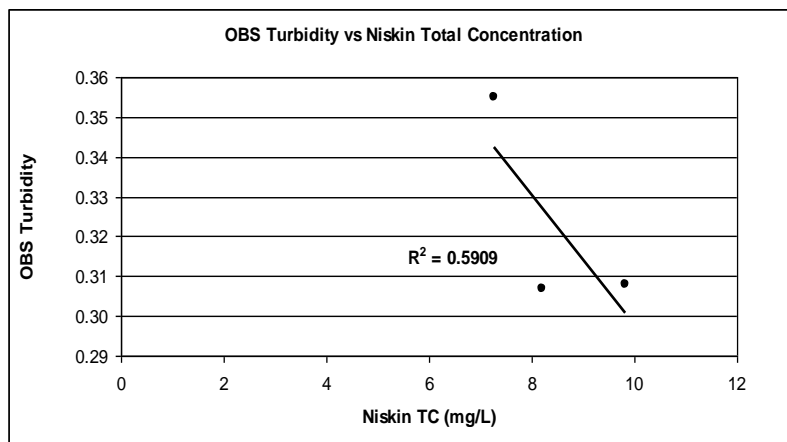


Fig. 4: Graph of OBS Turbidity Vs Niskin Total Concentration

**C. Turbidity and Bed Shear Stress**

Figure 5 shows a graph of the OBS turbidity values plotted against the calculated bed shear stress from Table 1. The two quantities are uncorrelated since the  $R^2$  value for the trend line

is so small, and  $\tau_0$  varies with no apparent relation to turbidity. It appears that turbidity does not affect  $\tau_0$ , in fact,  $\tau_0$  varies directly only with flow velocity.

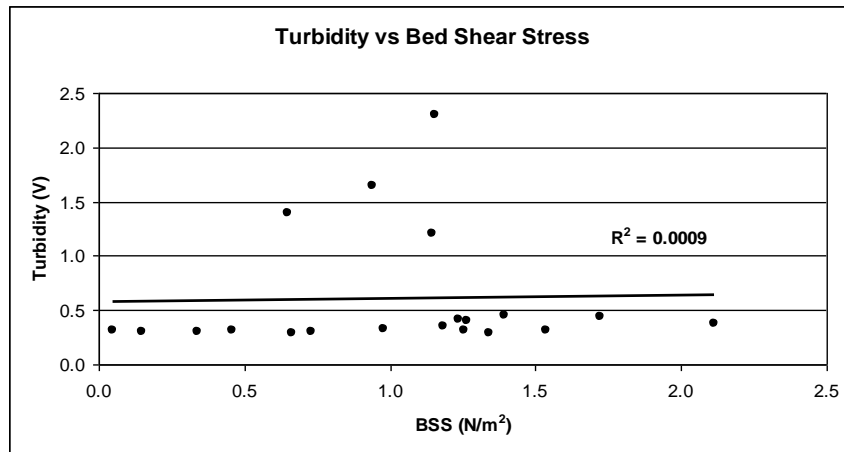


Fig. 5: Graph of OBS Turbidity Vs Bed Shear Stress

**D. Velocity Profiles**

Of the twenty velocity profiles examined, only nine had the appearance of the profile in Figure 1 and produced the log-linear line of Figure 2 from a trend line with  $R^2 \geq 0.95$ .

The other eleven had no log-linear shape because the water column was stratified, and the flow was not unidirectional when the ADCP recorded those profiles. Two such profiles are shown:

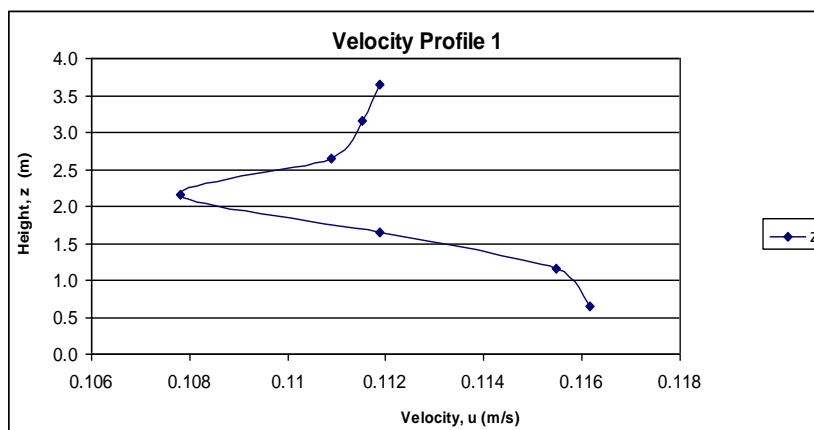


Fig. 6(a): Graph of Height above Bed Vs Flow Velocity

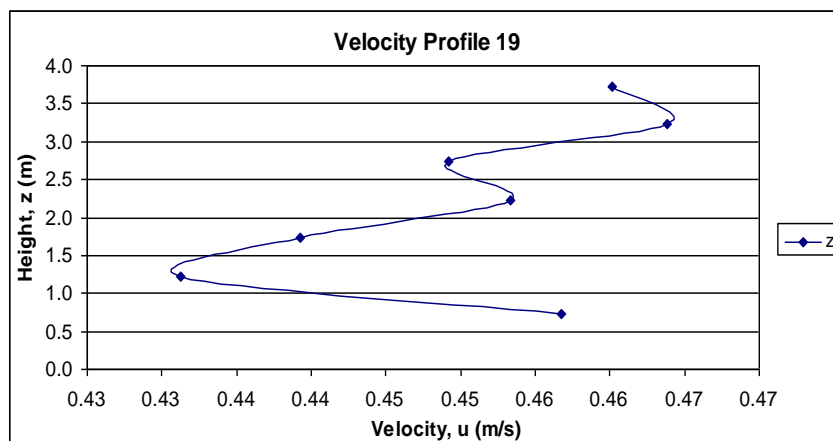


Fig. 6(b): Graph of Height above Bed Vs Flow Velocity

The nine log-linear profiles are reproduced below from Figure 7a to Figure 9c.

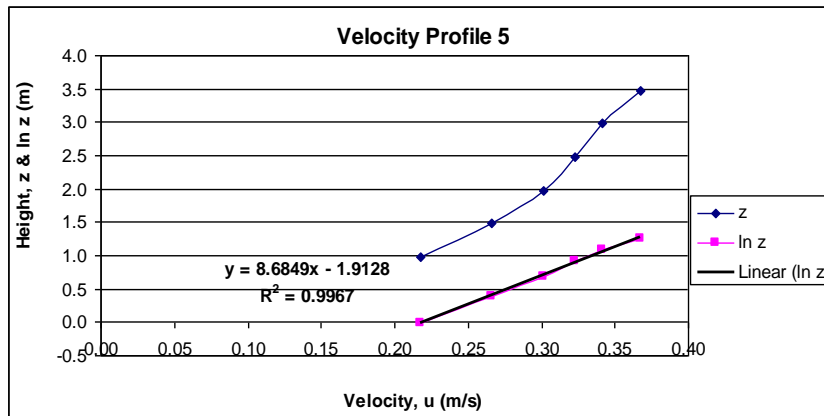


Fig. 7(a): Log-linear velocity profile with  $R^2 = 0.9967$

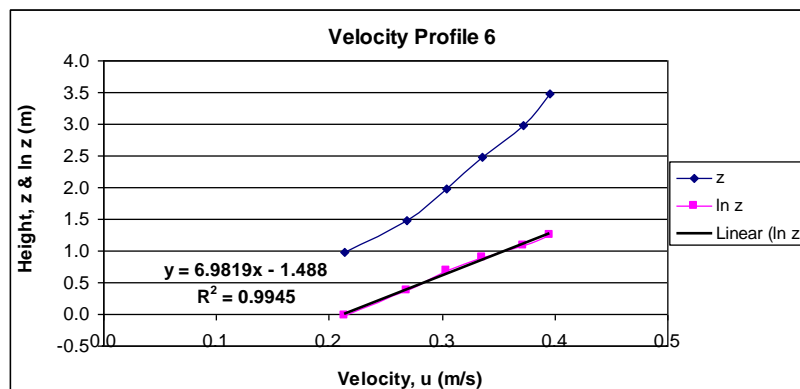


Fig. 7(b): Log-linear velocity profile with  $R^2 = 0.9945$

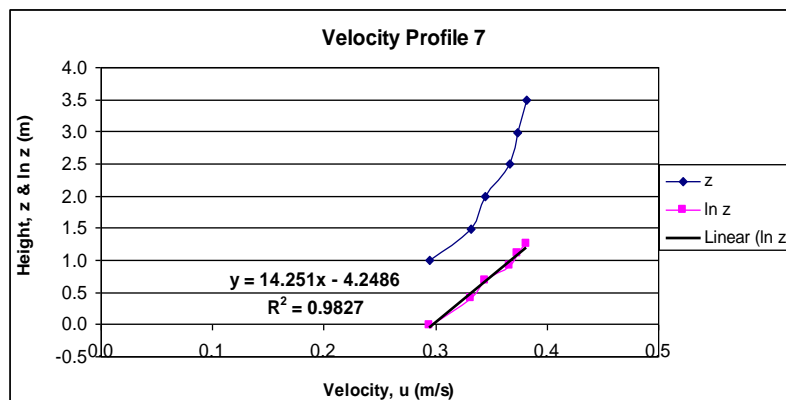


Fig. 7(c): Log-linear velocity profile with  $R^2 = 0.9827$

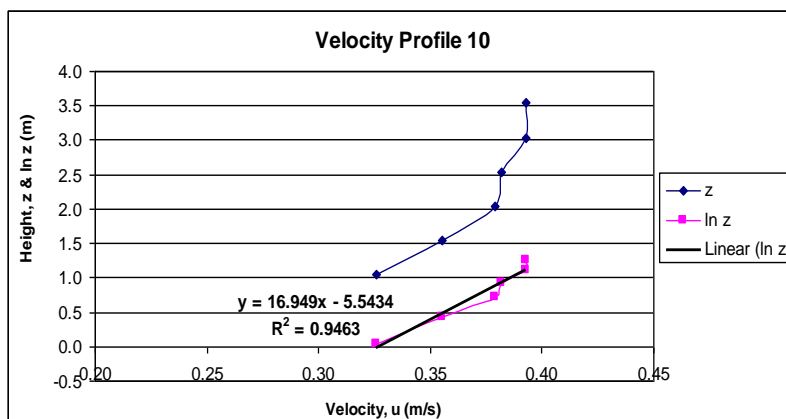


Fig. 8(a). Log-linear velocity profile with  $R^2 = 0.9463$

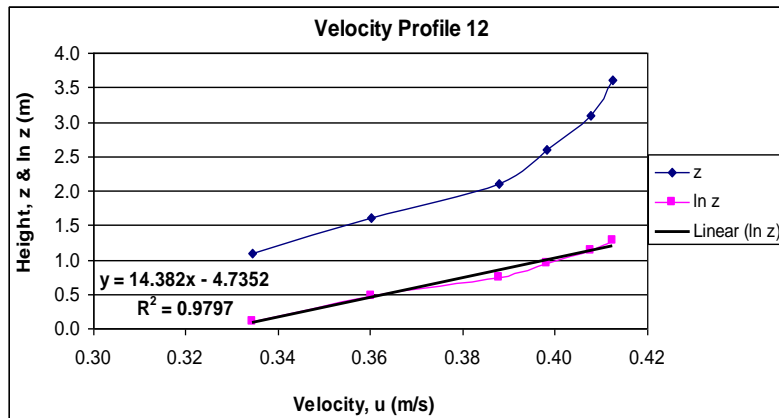


Fig. 8(b): Log-linear velocity profile with  $R^2 = 0.9797$

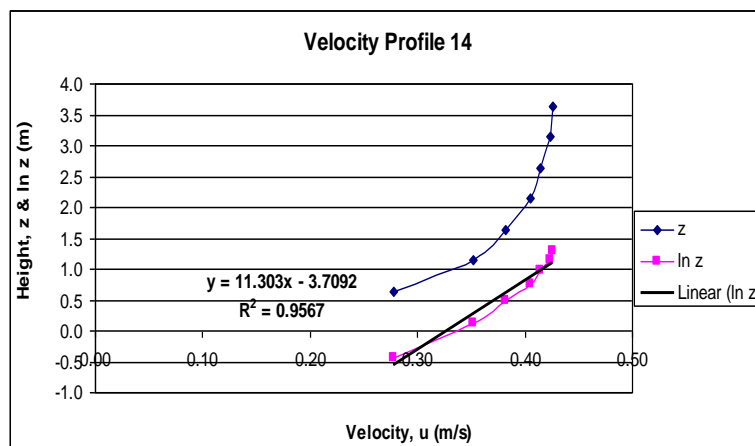


Fig. 8(c): Log-linear velocity profile with  $R^2 = 0.9567$

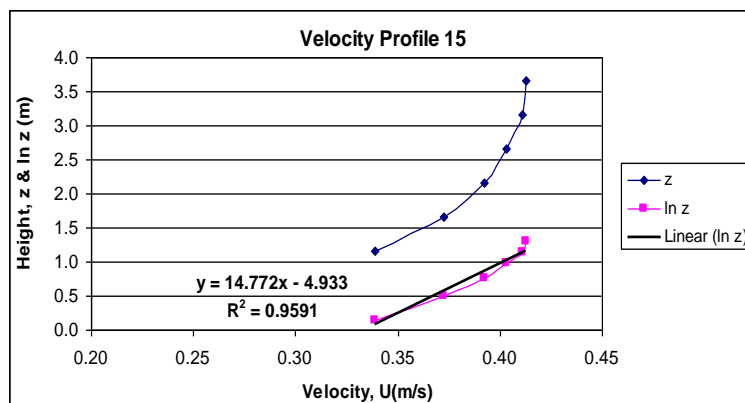


Fig. 9(a): Log-linear velocity profile with  $R^2 = 0.9591$

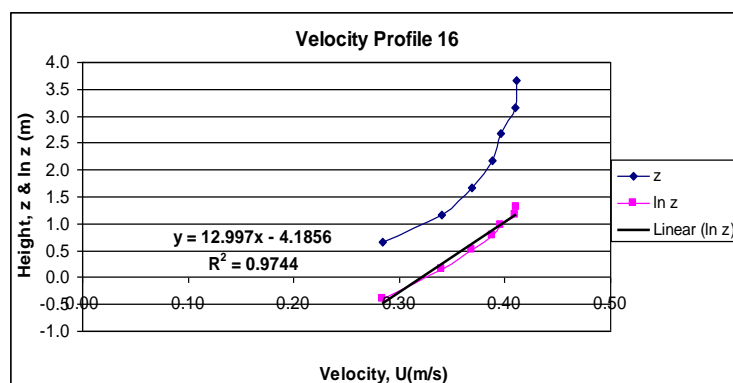


Fig. 9(b): Log-linear velocity profile with  $R^2 = 0.9744$



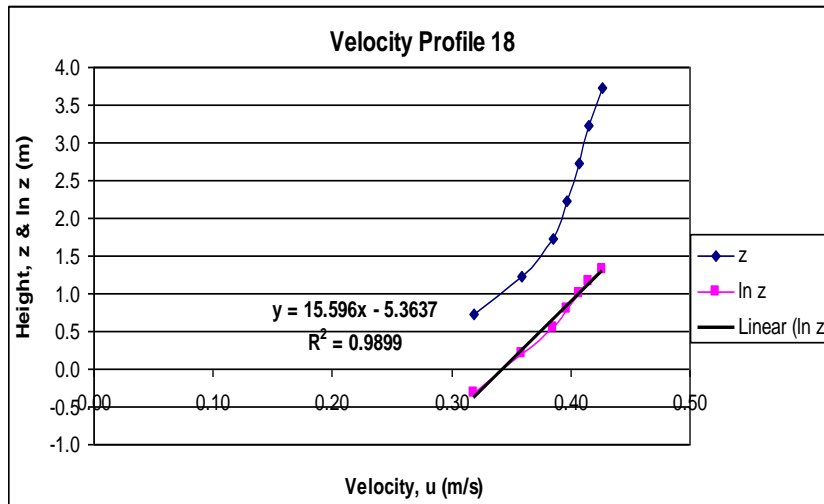


Fig. 9(c): Log-linear velocity with  $R^2 = 0.9899$

E. Evaluation of  $\kappa$  from Log-Linear Velocity Profiles & Comparison with Turbidity (SSC)  
 The gradient for each log-linear graph was obtained from

the given trend line equation and, with the corresponding friction velocity, used to find a value for von Karman's constant.

Table 3: Data for the Nine Selected Velocity Profiles

| Velocity Profile No. | Gradient $m$ | Friction velocity $u_*$ (m/s) | von Karman's $\kappa$ | OBS Turbidity (V) |
|----------------------|--------------|-------------------------------|-----------------------|-------------------|
| 5                    | 8.6849       | 0.027                         | 0.234                 | 0.307             |
| 6                    | 6.9819       | 0.025                         | 0.175                 | 0.295             |
| 7                    | 14.251       | 0.036                         | 0.513                 | 0.289             |
| 10                   | 16.949       | 0.034                         | 0.576                 | 0.355             |
| 12                   | 14.382       | 0.039                         | 0.561                 | 0.317             |
| 14                   | 11.303       | 0.041                         | 0.463                 | 0.436             |
| 15                   | 14.772       | 0.035                         | 0.396                 | 0.419             |
| 16                   | 12.997       | 0.037                         | 0.547                 | 0.451             |
| 17                   | 15.596       | 0.033                         | 0.515                 | 1.212             |

Avg  $\kappa = 0.442$ ; St. Dev. of  $\kappa = 0.138$ ; Range of  $\kappa = 0.175$  to  $0.576$

A graph of  $\kappa$  versus turbidity is shown below in Figure 10 along with the trend line and coefficient of determination,  $R^2$ .

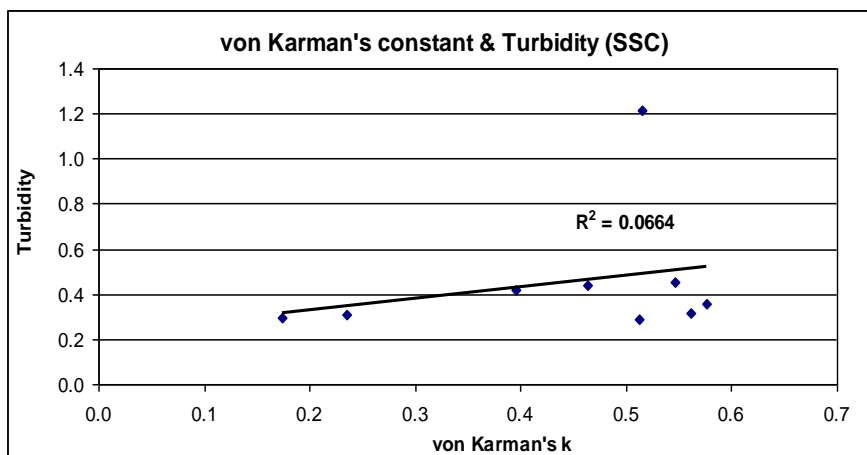


Fig. 10: Graph showing von Karman's  $\kappa$  Vs Turbidity

## IX. DISCUSSION

The values for friction velocity found using the adaptation of the Reynolds stress method are well within the order of magnitudes known in the literature, for example,  $u^* = 0.083$  m/s (Open University, 1989). This indicates that the Reynolds stress method is a fairly accurate in finding an independent value of the friction velocity.

The values found for von Karman's  $\kappa$  are similarly within the order of magnitude of the generally accepted value of 0.41 and the range (0.36 – 0.417) mentioned by Yalin (1972). The average value found, 0.442, is slightly more than 0.41, and given the standard deviation of 0.138 and instrumental-experimental errors, this is reasonable.

Still not fully settled is the question of the dependence of  $\kappa$  on suspended sediment concentration, as the trend line of Figure 10 gives a very low  $R^2$  value. In fact, the graph indicates that the variations of  $\kappa$  seem to be independent of turbidity. Also, the graph bears a close resemblance to the turbidity versus bed shear stress graph of Figure 5 and the  $R^2$  value is similarly very small. This is because  $\kappa$  and  $\tau_0$  are related in this manner: Given the gradient of the log-linear graph,  $m = \kappa/u^*$  and  $\tau_0 = \rho(u^*)^2$ , a simple mathematical combining arrives at  $\tau_0 = \rho(\kappa/m)^2$ .

## X. CONCLUSION

Once more, this shows that von Karman's constant is closely related to the bed shear stress, which results from the momentum flux of the flow being delivered into the bed.

However, the question of whether von Karman's constant is a robust constant or a weak variable that is affected by suspended sediment or some other factors is still not fully answered. There is, therefore, scope for further research.

## ACKNOWLEDGEMENT

Thanks to Prof. Carl Amos and Dr. Charlotte Thompson of the University of Southampton, National Oceanography Centre for advice and guidance.

Thanks also to the University for the use of the coastal vessel and laboratory facilities and for providing all the necessary technical support.

Finally, thanks to Ms. Ashmini Prasad, English Assistant Mistress of the Tagore Memorial Secondary School, Guyana, for assisting in completing and proofreading the manuscript.

## REFERENCES

- [1.] Bagnold, R.A. (1941, new ed. 1973). The physics of blown sand and desert dunes, Chapman & Hall Ltd., London. pp 50 – 51.
- [2.] Bergmann, J. C. (1998). A physical interpretation of von Karman's constant based on asymptotic considerations – A New Value. Journal of Atmospheric Sciences, Boston, pp 3404 – 3405.

- [3.] Cloutier, D., Amos, C. *et al.* (2006). The effects of suspended sediment concentration on turbulence in an annular flume. Aquatic Ecology **40**, pp 555–565. <https://doi.org/10.1007/s10452-005-4810-2>.
- [4.] Dyer, K. R. (1986). Coastal and estuarine sediment dynamics, John Wiley & Sons Ltd., Chichester. pp 49 – 50, 162
- [5.] Leeder, M. R. (1982). Sedimentology process and product, Unwin Hyman Ltd., London. pp 55 – 56
- [6.] Muir Wood, A. M. and Fleming, C. A. (1981). Coastal hydraulics, The Macmillan Press Ltd., London. p 12
- [7.] Open University. Oceanography Course Team. (1989). Waves, tides and shallow-water processes, Pergamon in association with the Open University, Oxford. p 79
- [8.] Soulsby, R. L. & Dyer, K.R. (1981). The form of near-bed velocity profiles in a tidally accelerating flow. Journal of Geophysical Research, UK. p 807
- [9.] Yalin, M.S. (1972). Mechanics of sediment transport, Pergamon Press Ltd., Oxford. p 22.